JACS
JOURNAL OF THE AMERICAN CHEMICAL SOCIETY
Article
pubs.acs.org/JACS

Reversible and Oriented Immobilization of Ferrocene-Modified Proteins

Lanti Yang,[†] Alberto Gomez-Casado,[†] Jacqui F. Young,[‡] Hoang D. Nguyen,[‡] Jordi Cabanas-Danés,[†] Jurriaan Huskens,[†] Luc Brunsveld,*[,‡] and Pascal Jonkheijm*[,†]

[†]Molecular Nanofabrication Group, Department of Science and Technology, MESA+ Institute for Nanotechnology, University of Twente, P.O. Box 217, 7500 AE Enschede, The Netherlands

[‡]Laboratory of Chemical Biology, Department of Biomedical Engineering, Eindhoven University of Technology, Den Dolech 2, 5612 AZ Eindhoven, The Netherlands

Supporting Information

ABSTRACT: Adopting supramolecular chemistry for immobilization of proteins is an attractive strategy that entails reversibility and responsiveness to stimuli. The reversible and oriented immobilization and micropatterning of ferrocene-tagged yellow fluorescent proteins (Fc-YFPs) onto β-cyclodextrin (βCD) molecular printboards was characterized using surface plasmon resonance (SPR) spectroscopy and fluorescence microscopy in combination with electrochemistry. The proteins were assembled on the surface through the specific supramolecular host−guest interaction between βCD and ferrocene. Application of a dynamic covalent disulfide lock between two YFP proteins resulted in a switch from monovalent to divalent ferrocene interactions with the βCD surface, yielding a more stable protein immobilization. The SPR titration data for the protein immobilization were fitted to a 1:1 Langmuir-type model, yielding $K_{LM} = 2.5 \times 10^5\ M^{-1}$ and $K_{i,s} = 1.2 \times 10^3\ M^{-1}$, which compares favorably to the intrinsic binding constant presented in the literature for the monovalent interaction of ferrocene with βCD self-assembled monolayers. In addition, the SPR binding experiments were qualitatively simulated, confirming the binding of Fc-YFP in both divalent and monovalent fashion to the βCD monolayers. The Fc-YFPs could be patterned on βCD surfaces in uniform monolayers, as revealed using fluorescence microscopy and atomic force microscopy measurements. Both fluorescence microscopy imaging and SPR measurements were carried out with the in situ capability to perform cyclic voltammetry and chronoamperometry. These studies emphasize the repetitive desorption and adsorption of the ferrocene-tagged proteins from the βCD surface upon electrochemical oxidation and reduction, respectively.

1. INTRODUCTION

The immobilization of proteins on chip surfaces plays an important role in various areas of biomedical and biotechnological research such as biomarker detection,[1] proteomic screens,[2] and drug discovery[3] and facilitates a systemic understanding of biological phenomena at the molecular level.[4] In addition, fields such as biosensor development[5] and tissue engineering,[6,7] which are not based directly on protein chips, nonetheless require controlled protein immobilization on substrates and materials.

Site-specific chemical strategies, as opposed to random attachment, provide precise control over immobilization of proteins in homogeneously oriented layers and coatings and yield improved performance.[8] For the immobilization of structurally sensitive proteins, chemical bonding with high specificity toward the protein of interest, mild reaction conditions compatible with the physiological milieu, and rapid as well as quantitative conversion are essential.[8] Exciting advances are currently being reported on a variety of bioorthogonal chemical transformations for site-specific covalent protein immobilization,[8,9] although most of these methods may lack responsiveness and reversibility.

Alternatively, the use of supramolecular chemistry to achieve adaptive biomimetic functions is an attractive strategy.[10,11] Supramolecular motifs employ well-established noncovalent interactions that are directional, reversible, and sensitive to environmental factors.[10] Although oriented protein immobilization approaches based on biological and synthetic supramolecular motifs have been reported in recent years,[12] it remains challenging to design supramolecular protein conjugates with functional groups that can orient proteins onto solid supports and are responsive to external stimuli.[13] A recent report by Grunwald et al.[13a] accomplished an autoinhibition strategy in which a surface-bound multivalent chelator head was tethered with an intramolecular ligand that could initially compete with and inhibit binding of His-tagged proteins. Conversely, binding was activated by a photoreaction separating the intramolecular ligand from the multivalent

Received: August 25, 2012
Published: November 3, 2012

   dx.doi.org/10.1021/ja308450n | J. Am. Chem. Soc. 2012, 134, 19199−19206

Scheme 1. (A) Cysteine-Functionalized Ferrocene (Fc) Is Coupled to Thioester-Functionalized Yellow Fluorescent Protein (YFP) To Give Site-Specifically Fc-Tagged YFP (Fc-YFP) Variants; (B) Covalent Locking (via Disulfide Formation) and Non-Covalent Locking (via Intrinsic Affinity) Yield Divalent Fc-YFP Variants Starting from Their Monovalent Counterparts; Two YFP Variants Are Used, One Prone To Dimerize (dYFP) and One Suppressed from Dimerization [Enhanced YFP (eYFP)]; (C) Thioether-Functionalized βCD Monolayers Are Self-Assembled on Gold Slides, and Variants of Fc-YFP Are Complexed to the βCD SAMs with Different Binding Affinities; Following Oxidation and Reduction of the Fc Groups, the Proteins Can Be Desorbed and (Re-)Adsorbed, Respectively (Abbreviations: SS, Disulfide Formation; S, Free Cysteine; SB, Cysteine Reacted with *N*-Methylmaleimide)

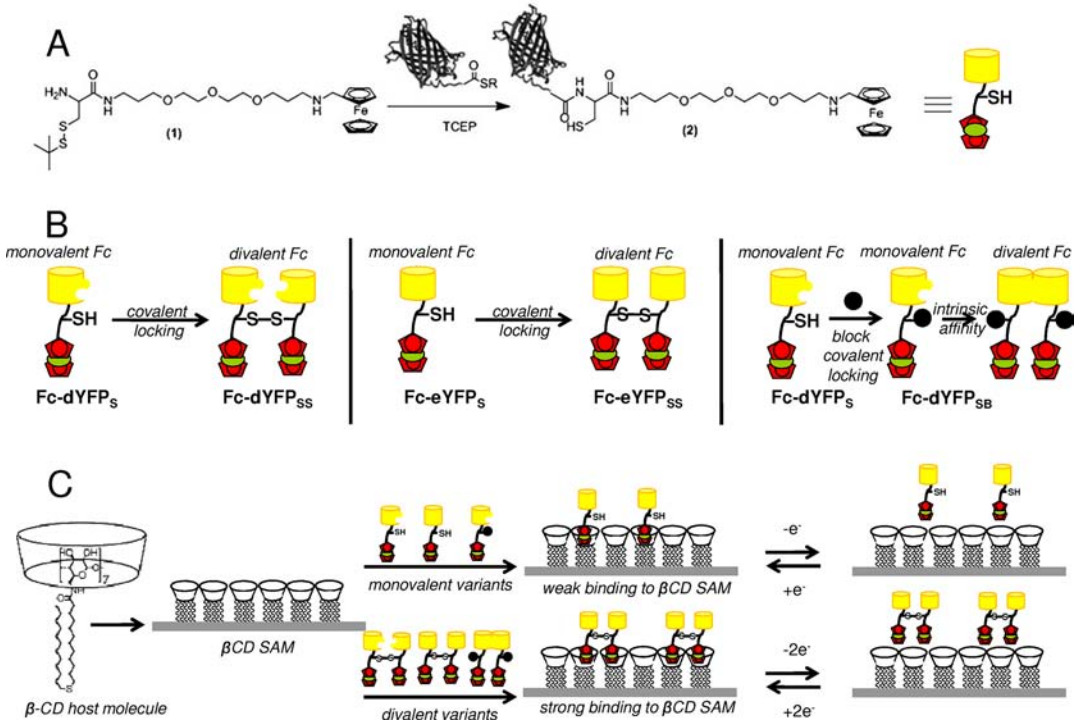

chelator head.[13a] Hyun et al.[13b] fabricated stimulus-responsive elastin-like polypeptide (ELP) nanostructures that undergo a switchable and reversible hydrophilic−hydrophobic phase transition at a lower critical solution temperature. This behavior was used as a switch for reversible immobilization of a thioredoxin−ELP fusion protein onto the ELP nanopatterns.[13b] Wan et al.[13c] designed a dual light- and pH-responsive biocompatible interface using the photocontrolled interaction between an azobenzene-functionalized self-assembled monolayer (SAM) and β-cyclodextrin (βCD)-functionalized pH-responsive poly(acrylic acid) polymers.

Because of the noninvasive and quantitative nature of redox reactions, electrochemically programmable interfaces functionalized with proteins hold considerable promise as responsive substrates.[10e,14,15] While a few of the above-mentioned supramolecular protein immobilization strategies have been documented in the literature, in cases where functional attachment of proteins to solid supports with dynamic properties has been realized, protein conjugates directly equipped with tags that are responsive to electrochemical stimuli are still required.[16]

In this work, we utilized site-selective incorporation of a ferrocene (Fc) guest moiety into a protein followed by oriented reversible immobilization onto a SAM of βCD host molecules. Supramolecular immobilization of Fc-modified proteins on SAMs of cucurbit[*n*]uril (CB[*n*], *n* = 7) has been reported.[12f,h] Ferrocenium (Fc^+) guests form highly stable 1:1 inclusion complexes with the supramolecular host CB[*n*] (*n* = 7, 8), which upon electrochemical reduction of the guest leads only to a modest loss in binding affinity on the order of a factor 10.[18] In strong contrast, the complexation of ferrocene with βCD is strongly diminished upon oxidation of Fc to Fc^+.[17] The redox behavior of Fc has been employed to control the positioning of molecules on βCD SAMs,[18] which has been demonstrated, for example, in the assembly of ferrocene-modified polymers,[19] dendrimers[20] and peptides.[21,22] The reported procedures, however, can seriously affect the three-dimensional structures and orientations of the proteins as a result of the utilization of acidic or organic milieus,[19−21] and the adopted strong multivalent interactions may hamper the reversibility of immobilization.[10f,19−22]

The Fc-βCD guest−host supramolecular method presented in Scheme 1 satisfies important requirements of protein array preparation, such as mildness, operation under buffered conditions, bio-orthogonality, specificity, and stable and reversible assembly. Furthermore, while the stability of the monovalent supramolecular Fc−βCD complex was relatively weak, we sought to stabilize the surface assemblies by employing intrinsic protein dimerization and covalent locking of protein dimers facilitated by the formation of a disulfide linkage (Scheme 1B).[23] Moreover, we demonstrate reversible properties of the protein assemblies upon applying an electrochemical stimulus to the surface assemblies (Scheme 1C).

dx.doi.org/10.1021/ja308450n | *J. Am. Chem. Soc.* 2012, 134, 19199−19206

2. RESULTS AND DISCUSSION

2.1. Materials. Fluorescent proteins were used in this study because they provide an intrinsic probe of the structural integrity of the proteins upon immobilization, as their fluorescence characteristics are highly sensitive to even minute changes in their native structure. To functionalize yellow fluorescent proteins (YFPs) with a supramolecular Fc tag, the site-selective technique of expressed protein ligation previously developed by us was adopted to connect a cysteine-modified ferrocenyl compound to the YFP (Scheme 1A).[12h,23] For the conjugation of cysteine-modified ferrocene (**1**) to the respective YFP thioesters, the protein and ferrocene derivatives were mixed in a reducing buffer in a 1:20 ratio. After overnight incubation on a rotating wheel at room temperature, the reactions were typically complete, and the excess ferrocene and reducing agent were removed, affording the pure protein constructs (**2**) (see the Supporting Information). Five different Fc-YFP constructs with different ferrocene valencies were generated by making use of the intrinsic affinity for homodimerization[23] and the oxidation state of a cysteine residue for covalent homodimerization (Scheme 1B).[24] The monovalent variant **Fc-dYFP$_S$** contained two mutations that increased the affinity for dimerization (S208F and V224L), while the enhanced variant **Fc-eYFP$_S$** did not have any dimerization-promoting mutations. As shown in Scheme 1A, the semisynthesis of the supramolecular Fc-YFPs resulted in the introduction of a cysteine (denoted by the S subscript), which was amenable to oxidation to form covalent disulfide cross-links (denoted by the SS subscript); this feature was used to generate divalent Fc-YFP constructs of both variants, i.e. **Fc-eYFP$_{SS}$** and **Fc-dYFP$_{SS}$** (Scheme 1B). In the last variant, **Fc-dYFP$_{SB}$**, the cysteine of the monovalent ferrocene was blocked by reaction with *N*-methylmaleimide (Scheme 1B). The different Fc-YFP variants were assembled on SAMs of βCD (Scheme 1C). To this end, βCD was modified with seven heptathioether chains to form highly ordered and densely packed SAMs on gold (so-called "molecular printboards").[25] βCD has a weak binding affinity for ferrocene in solution (K_a on the order of 10^3 M^{-1}).[26] The intrinsic binding constant of ferrocene to a single surface-bound βCD cavity was found to be comparable to the intrinsic binding constant of these molecules to βCD in solution.[27]

In this way, we envisaged the possibility of tuning the weak supramolecular interaction between Fc and βCD into stable assemblies as a result of the favorable binding between the proteins. Moreover, we thought it would be possible to reverse the assembly of Fc-YFPs onto the βCD SAM using an electrochemical oxidation trigger as an external stimulus (Scheme 1C).

2.2. Self-Assembly. To gain insight into the self-assembly of the ferrocene-tagged YFP constructs onto βCD SAMs, surface plasmon resonance (SPR) reflectivity measurements were performed at a constant angle. In all of the SPR experiments to follow, 1 mM Tween-20 was added to the buffer to suppress any flow-induced physical adsorption of the proteins to βCD SAMs (see Figure S1 in the Supporting Information). No binding was observed when a control YFP without a ferrocene tag was used at a concentration of 60 μM, which was 2-fold higher than the highest concentration used for any of the experiments with Fc-functionalized proteins. However, clear binding events in the SPR signal were observed in the case of all five Fc-YFP constructs (Figure 1). These results indicated that the assembly of YFP occurred specifically through the Fc–βCD guest–host motif, as envisioned (Scheme 1C).

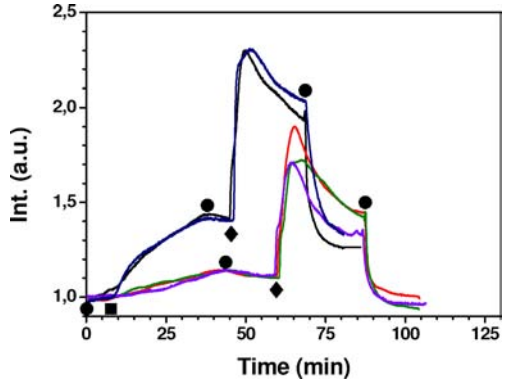

Figure 1. SPR responses monitoring the adsorption and desorption of the Fc-YFP constructs depicted in Scheme 1B (10 μM) on βCD SAMs. Symbols indicate switching of solutions in the SPR flow cell: (●) buffer 1 or 2; (■) 10 μM protein in buffer 1 or 2; (◆) 10 mM βCD in buffer 1 or 2. Curves: (black) **Fc-dYFP$_{SS}$** in buffer 1; (red) **Fc-dYFP$_S$** in buffer 2; (green) **Fc-dYFP$_{SB}$** in buffer 1; (blue) **Fc-eYFP$_{SS}$** in buffer 1; (violet) **Fc-eYFP$_S$** in buffer 2. Buffer 1: PBS with 1 mM Tween-20. Buffer 2: buffer 1 + 2 mM TCEP.

When the SPR sensorgrams of **Fc-dYFP$_S$** and **Fc-eYFP$_S$** at equal concentration (10 μM) in a a reducing buffer containing 2 mM tris(2-carboxyethyl)phosphine (TCEP) were compared, no differences in the association were observed (Figure 1, red and violet curves). This association behavior was in strong contrast to the case where these protein constructs were assembled using a buffer without the reducing agent. As shown by the black and blue curves in Figure 1, both of the covalently cross-linked constructs **Fc-dYFP$_{SS}$** and **Fc-eYFP$_{SS}$** exhibited higher adsorption to the surface. The difference between the monovalent and divalent Fc-YFP constructs was also visible upon rinsing with 10 mM βCD for 25 min (Figure 1). After a sudden increase in SPR signal due to the large change in refractive index caused by adding a concentrated solution of βCD, a clear loss in the SPR signal was observed during the rinsing, which was steeper in the case of the monovalent Fc-YFPs. After this step, the flow was switched back to the original running buffer, and the baseline was restored only in the case of the monovalent Fc-YFPs, whereas a significant residual protein adsorption was observed after a similar rinsing time when the divalent ferrocene-tagged YFPs were used. These results indicate that the interaction between the Fc-tagged YFPs and the surface was reversible for both the mono- and divalent Fc variants, with the latter variants being bound more tightly to the host surface. To test whether the intrinsic affinity of **Fc-dYFP$_S$**, which would lead to the formation of divalent Fc-YFP, would make a measurable contribution to the stability of the surface assemblies, an SPR experiment was performed with 10 μM **Fc-dYFP$_{SB}$**, in which the thiol groups were blocked by reaction with *N*-methylmaleimide to prevent the formation of a disulfide bridge. In this case, the SPR response during assembly and disassembly was comparable with those of the two monovalent YFP variants (Figure 1, green curve).

Taken together, these SPR results are in line with our hypothesis that the weak interaction of the monovalent Fc-YFPs with βCD can be stabilized through covalent protein dimerization to give a divalent Fc-YFP construct. When this covalent locking was prevented, the mutation sites on dYFP

dx.doi.org/10.1021/ja308450n | J. Am. Chem. Soc. 2012, 134, 19199–19206

were found not to assist in stabilizing the YFP interaction with the βCD SAM.

To shed more light on the valency of the interaction between Fc-YFP and the βCD surface, SPR titrations were performed by adding solutions with different concentrations of covalently cross-linked **Fc-eYFP$_{SS}$** to βCD SAMs (Figure 2). The SPR

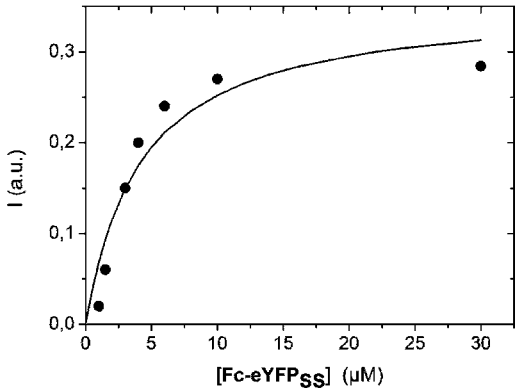

Figure 2. SPR titration (●) and corresponding fit to a 1:1 Langmuir-type model (solid line) for the binding of **Fc-eYFP$_{SS}$** to a βCD SAM in PBS containing 1 mM Tween-20.

data were fitted to a 1:1 Langmuir-type model, which assumes that the two ferrocene moieties of **Fc-eYFP$_{SS}$** simultaneously interact with CD cavities at the surface (see the Supporting Information for details). As shown in Figure 2, the SPR data were satisfactorily fitted to yield an overall binding constant (K_{LM}) of 2.5×10^5 M^{-1} for **Fc-eYFP$_{SS}$**. The overall binding constant can be related to the intrinsic binding constant at the surface for monovalent Fc–βCD interaction ($K_{i,s}$) and the maximum effective concentration at the surface ($C_{eff,max}$), as shown in eq 1:[28]

$$K_{LM} = C_{eff,max}(K_{i,s})^2 \quad (1)$$

With $C_{eff,max}$ = 0.2 M,[28] $K_{i,s}$ was calculated to be 1.2×10^3 M^{-1}, which matches the $K_{i,s}$ value of 1.2×10^3 M^{-1} presented in the literature for the interaction of monovalent Fc with βCD SAMs in the case of small molecules.[27] This indicates that the proteins and the buffer composition did not influence the Fc–βCD binding affinity. The overall binding constant K_{LM} for the divalent Fc–βCD interaction is 2 orders of magnitude higher than $K_{i,s}$ and is in agreement with the observations described above that more stable binding was found between the divalent ferrocene-tagged protein and the βCD surface. Similar values were achieved when βCD SAMs were titrated with **Fc-dYFP$_{SS}$**. These results confirmed that a divalent ferrocene–βCD interaction occurs in the assembly of the Fc-YFP constructs onto βCD SAMs.

2.3. SPR Simulation. Obtaining a direct estimation of the monovalent Fc-YFP affinity with the βCD SAM was hampered by the impractically high concentrations (mM range) required to perform a reliable SPR titration of monovalent **Fc-eYFP$_S$** or **Fc-dYFP$_S$** (in the presence of a reducing agent). Therefore, a computer simulation of the SPR experiments was performed. For the YFP constructs with mono- and divalent ferrocene binding modes to the βCD SAM, both the assembly and the disassembly were simulated. The disassembly was simulated in the case of washing with host competitor βCD present in the buffer. As shown in Figure 3, in phase I, the adsorption of 10 μM Fc-YFP in the divalent mode covers ~16% of the βCDs of

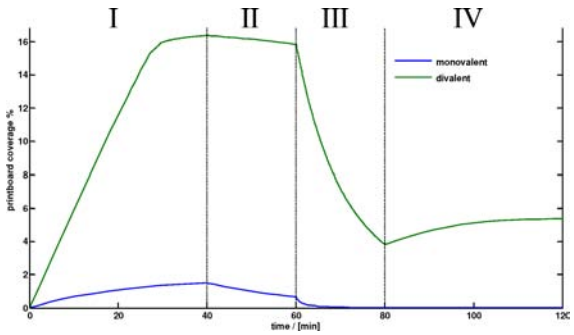

Figure 3. Simulation of the SPR experiments. Phase I: injection of a solution of 10 μM Fc-YFP protein for 40 min. Phase II: injection of buffer for 20 min. Phase III: injection of a solution of 10 mM βCD for 20 min. Phase IV: injection of buffer for 20 min. Details of the simulation procedure are given in the Supporting Information.

the SAM, whereas Fc-YFP in the monovalent mode shows a much lower adsorption of ~2% of the βCD SAM, which is analogous to the experimental SPR sensorgrams (Figure 1). Because of the steric effect of YFP, the theoretical full coverage of Fc-YFP on βCD is $\sim 1.3 \times 10^{-11}$ mol/cm^2, which is indeed 16% of the coverage of the βCD SAM (8×10^{-11} mol/cm^2).[25,28] These results imply that the YFP constructs equipped with two ferrocene moieties cover the βCD SAM more rapidly and to the maximum extent compared with the monovalent Fc-YFPs. The surface coverage of the ferrocene groups on the βCD monolayer was confirmed by integrating the cyclic voltammetry (CV) scans; this gave a value of 1.4×10^{-11} mol/cm^2 (see Figure S2 in the Supporting Information), which is in accordance with the simulated value. As shown in Figure 3, in phase III, upon addition of 10 mM βCD to the solution as a competitor to binding with the βCD SAM, the baseline was not restored in the case of divalent Fc-YFP but was completely restored in the case of monovalent Fc-YFP. Although the desorption of the proteins was visible in both the experiments and simulations, the large change in refractive index induced by the high concentration of βCD was not simulated. Taken together, the simulation agreeably describes the SPR experiments, supporting the surface assembly of mono- and divalent ferrocene-tagged proteins by tuning the oxidation state of the cysteine.

2.4. Visualization of Protein Assemblies. To visualize the protein assemblies using fluorescence microscopy and atomic force microscopy (AFM), the stronger-binding dimeric protein constructs were selected for patterning employing the well-established microcontact printing (μCP) method with a polydimethylsiloxane (PDMS) stamp.[29] Such stamps were inked for 10 min with a 10 μM solution of divalent **Fc-eYFP$_{SS}$** in phosphate-buffered saline (PBS). After inking, the stamp was blown dry and put into conformal contact with a βCD SAM on gold for 15 min. After subsequent rinsing with a large amount of PBS and water, the slide was imaged. As a reference, similar experiments were performed in which the PDMS stamp was inked with a 60 μM solution of YFP without the ligated ferrocene guest moiety. Uniform patterns of Fc-YFP were clearly visible, as imaged using fluorescence microscopy (Figure 4A). In contrast, no patterns were observed when the control YFP protein without the ferrocene linker was applied (Figure 4B). After an overnight rinse with βCD, the patterns disappeared, which is characteristic of reversible supramolecular interactions between the proteins and the surface. The

dx.doi.org/10.1021/ja308450n | J. Am. Chem. Soc. 2012, 134, 19199–19206

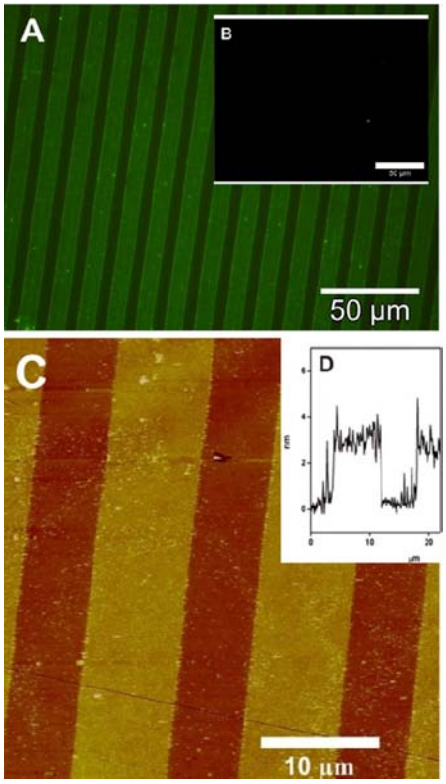

Figure 4. Fluorescence microscopy images of (A) **Fc-eYFP$_{SS}$** and (B) control YFP without Fc at the βCD SAM patterned by μCP after rinsing with PBS and water. (C) AFM image of the patterned **Fc-eYFP$_{SS}$** and (D) line scan along the **Fc-eYFP$_{SS}$** pattern.

patterned Fc-YFP layers on the βCD SAM were also characterized using tapping-mode AFM experiments (Figure 4C). The height of Fc-YFP was measured to be 3.0 ± 0.2 nm (Figure 4D), which is consistent with the width of the YFP barrel.[30] The observations made by fluorescence microscopy and AFM suggest that the monolayers of homogeneously oriented proteins were fabricated as governed by the specific and reversible host–guest interactions.

2.5. Electrochemically Controlled Assembly. To investigate the redox-responsive behavior of the divalent **Fc-eYFP$_{SS}$** proteins assembled on the supramolecular βCD SAM on gold, an electrochemical signal was used as a mild external control for the reversible binding of Fc-YFP on the βCD surface. The desorption and readsorption of Fc-YFP on βCD SAMs was first visualized using fluorescence microscopy while performing in situ electrochemical experiments. Next, further characterization was done using SPR monitoring with in situ CV measurements.

Fluorescence imaging with in situ electrochemistry was performed on βCD SAMs with homogeneous 100 μm × 100 μm lines of **Fc-eYFP$_{SS}$**, which were prepared on gold surfaces by μCP as described above. The substrates were then mounted in a liquid cell equipped for electrochemistry experimentation. Fluorescence images of the patterned **Fc-eYFP$_{SS}$** were recorded while the liquid cell was filled with buffer.

Figure 5A1–D1 shows a series of fluorescence images of **Fc-eYFP$_{SS}$** during CV scans, which are presented in Figure 6A. Both the fluorescence intensity and the oxidation peak intensity decreased gradually after every CV scan, indicating the release of the proteins from the surface. When the ferrocenyl groups are oxidized to ferrocenium cations, they no longer form inclusion complexes with βCD, leading to desorption of the ferrocene-tagged proteins from the βCD surface and diffusion into solution. Because of the large volume of solution for the CV measurements, only Fc-YFPs remaining close to the surface could readsorb to the surface during subsequent reduction, resulting in a continuously decreasing intensity of the redox peaks. Another patterned surface with **Fc-eYFP$_{SS}$** was subjected to chronoamperometry (CA) experiments with simultaneous fluorescence microscopy imaging. After a potential step of +0.3 V was imposed, the ferrocenyl groups were oxidized to ferrocenium cations. This resulted in full dissociation of **Fc-eYFP$_{SS}$** from the βCD surface, as indicated by the decrease of the oxidation current to zero (Figure 6B). As shown in the Figure 6B inset, the recorded current was found to decay continuously in time, and a plot of its value versus $t^{-0.5}$ was linear, as expected for rapid processes in which the current is diffusion-limited.[31] The in situ fluorescence images (Figure 5A2–D2) show a significant decrease in fluorescence intensity after just a few seconds of CA, which suggests that the majority of ferrocene-tagged proteins were desorbed from the βCD monolayer within this period.

To investigate further the electrochemical desorption and readsorption of **Fc-eYFP$_{SS}$** on βCD SAMs, CV measurements

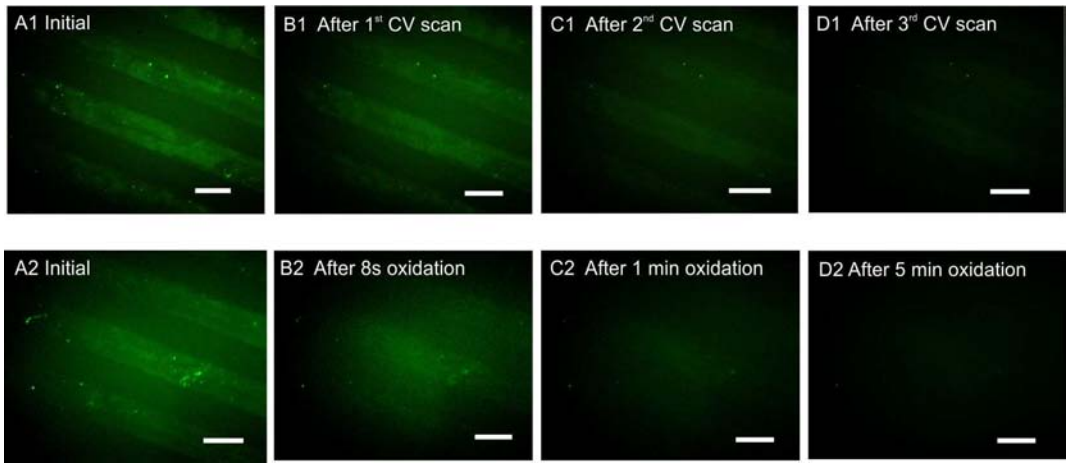

Figure 5. in-situ fluorescence images of patterned **Fc-eYFP$_{SS}$** on βCD monolayers upon (A1–D1) cyclic voltammetry or (A2–D2) chronoamperometric oxidation. The scale bars in all images represent 100 μm.

dx.doi.org/10.1021/ja308450n | J. Am. Chem. Soc. 2012, 134, 19199–19206

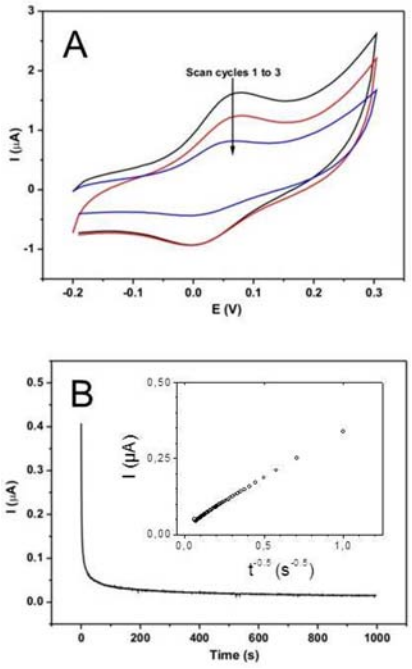

Figure 6. In situ-recorded (A) CV scans and (B) CA scan during fluorescence microscopy imaging. A Cottrell plot is given in the inset of (B).

were performed while the SPR response was recorded. As shown in Figure 7, a decrease in the SPR reflectivity was

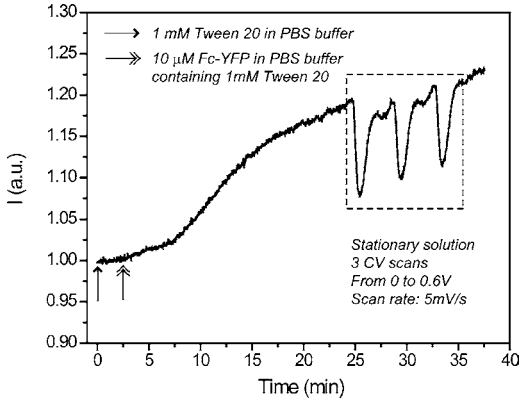

Figure 7. SPR response of a βCD SAM upon assembly of 10 μM **Fc-eYFP$_{SS}$** in PBS with 1 mM Tween-20 while performing CV at a scan rate of 5 mV/s (dashed box).

recorded from the moment that the onset of the oxidation potential was passed. As the oxidation peak potential was passed, the SPR signal kept on decreasing while Fc groups were oxidized. This observation indicates the desorption of Fc-YFPs away from the βCD SAM and is in agreement with the results of the fluorescence imaging experiments. When the potential was gradually changed to below the reduction peak potential during the backward part of the CV cycle, an increase in the SPR reflectivity was observed. This result indicates the readsorption of Fc-YFPs on the βCD SAM from the stationary solution in the liquid cell above the βCD SAM. The readsorption of Fc-YFP continued until the onset of the oxidation peak potential of the subsequent CV scan was reached. The cycle of adsorption and desorption could be repeated as long as CV measurements were performed. Three such repetitive CV scans are presented in the dashed box in Figure 7; they show similar increases in SPR signal between reduction and oxidation and similar decreases between oxidation and reduction. With a scan rate of 5 mV/s, the time between oxidation and reduction was sufficient to allow the reformation of a complete monolayer of Fc-YFP on the βCD SAM between scans, while 5 mV/s allowed for the desorption of 60−70% of the Fc-YFPs upon oxidation as estimated from the loss in SPR signal. The combined results show the reversible immobilization of Fc-YFPs onto a βCD SAM using a specific electrochemical signal as an external stimulus.

3. CONCLUSIONS

We have developed a supramolecular method for orientationally controlled immobilization of site-specifically ferrocene-modified proteins onto βCD-modified surfaces. Characterization using SPR experiments and simulations showed that the proteins self-assemble specifically and through monovalent and divalent ferrocene interactions at the βCD interface. Covalent locking of two proteins by disulfide formation created a divalent ferrocene-tagged protein construct that bound with an overall binding constant of 2.5×10^5 M^{-1} and an intrinsic binding constant of 1.2×10^3 M^{-1}, the latter of which is in agreement with the binding constant found in the case of small-molecule ferrocene−βCD binding at the surface. The divalent ferrocene-tagged protein was successfully used to fabricate uniform fluorescent patterns with a thickness of one protein molecule, as visualized using fluorescence microscopy and atomic force microscopy. Reversible protein immobilization was demonstrated upon oxidation of the ferrocene moieties.

The results of this study describe a biomimetic system that merges the possibilities of controlling the orientation, valency, affinity, reversibility, and responsiveness. Such systems are currently of interest for fabricating adaptive biomimetic interfaces.[32] Accessibility to protein biosurfaces to intervene with spatial and temporal resolution is important in, for example, detailed studies of biological processes at the cellular level.

■ ASSOCIATED CONTENT

Ⓢ Supporting Information

Experimental methods, model, SPR simulation, control SPR experiments using YFP without the Fc tag in buffer with/without Tween-20 (Figure S1), and CV to determine the surface coverage (Figure S2). This material is available free of charge via the Internet at http://pubs.acs.org.

■ AUTHOR INFORMATION

Corresponding Author

l.brunsveld@tue.nl; p.jonkheijm@utwente.nl

Notes

The authors declare no competing financial interest.

■ ACKNOWLEDGMENTS

The work by L.Y. and P.J. was funded by a starting grant from the European Research Council (ERC) (259183 Sumoman) and a VENI Grant (700.57.401) from the Council of the Chemical Sciences of the Dutch Science Foundation. A.G.-C. was supported by the Dutch Nanotechnology Network (NanoNed Project TPC 6939 to J.H.). J.F.Y., H.D.N., and

L.B. were supported by an ERC starting grant (204554 SupraChemBio). L.B and P.J. gratefully acknowledge Project P4.02 Superdices of the research program of the BioMedical Materials Institute, cofunded by the Dutch Ministry of Economic Affairs, Agriculture, and Innovation. J. Song is acknowledged for assistance with setting up the electrochemical liquid cell. C. Nicosia is acknowledged for artwork.

REFERENCES

(1) (a) Hudson, M. E.; Pozdnyakova, I.; Haines, K.; Mor, G.; Snyder, M. *Proc. Natl. Acad. Sci. U.S.A.* **2007**, *104*, 17494−9. (b) Zhu, H.; Hu, S. H.; Jona, G.; Zhu, X. W.; Kreiswirth, N.; Willey, B. M.; Mazzulli, T.; Liu, G. Z.; Song, Q. F.; Chen, P.; Cameron, M.; Tyler, A.; Wang, J.; Wen, J.; Chen, W. J.; Compton, S.; Snyder, M. *Proc. Natl. Acad. Sci. U.S.A.* **2006**, *103*, 4011−6. (c) Anderson, K. S.; Ramachandran, N.; Wong, J.; Raphael, J. V.; Hainsworth, E.; Demirkan, G.; Cramer, D.; Aronzon, D.; Hodi, F. S.; Harris, L.; Logvinenko, T.; LaBaer, L. *J. Proteome Res.* **2008**, *7*, 1490−9.

(2) (a) Dufva, M.; Christensen, C. B. *Expert Rev. Proteomics* **2005**, *2*, 41−8. For examples, see: (b) Jones, R. B.; Gordus, A.; Krall, J. A.; MacBeath, G. *Nature* **2006**, *439*, 168−74. (c) Kaushansky, A.; Gordus, A.; Budnik, B. A.; Lane, W. S.; Rush, J.; MacBeath, G. *Chem. Biol.* **2008**, *15*, 808−17. (d) Gong, W.; He, K.; Covington, M.; Dinesh-Kumar, S. P.; Snyder, M.; Harmer, S. L.; Zhu, X.-Y.; Deng, X. W. *Mol. Plant* **2008**, *1*, 27−41.

(3) (a) Terstappen, G. C.; Schlupen, C.; Raggiaschi, R.; Gaviraghi, G. *Nat. Rev. Drug Discovery* **2007**, *6*, 891−903. (b) Huang, J.; Zhu, H.; Haggarty, S. J.; Spring, D. R.; Hwang, H.; Jin, F.; Snyder, M.; Schreiber, S. L. *Proc. Natl. Acad. Sci. U.S.A.* **2004**, *101*, 16594−9. (c) Sokolov, B. P.; Cadet, J. L. *Neuropsychopharmacology* **2006**, *31*, 956−66.

(4) (a) Phizicky, E.; Bastiaens, P. I. H.; Zhu, H.; Snyder, M.; Fields, S. *Nature* **2003**, *422*, 208−15. (b) Weinrich, D.; Jonkheijm, P.; Niemeyer, C. M.; Waldmann, H. *Angew. Chem., Int. Ed.* **2009**, *48*, 7744−51. (c) Predki, P. F. *Curr. Opin. Chem. Biol.* **2004**, *8*, 8−13. (d) Niemeyer, C. M. *Trends Biotechnol.* **2002**, *20*, 395−401. (e) Zhu, H.; Snyder, M. *Curr. Opin. Chem. Biol.* **2003**, *7*, 55−63.

(5) (a) Martinez, A. W.; Phillips, S. T.; Whitesides, G. M. *Proc. Natl. Acad. Sci. U.S.A.* **2008**, *105*, 19606−11. (b) Schroeder, H.; Adler, M.; Gerigk, K.; Müller-Chorus, B.; Götz, F.; Niemeyer, C. M. *Anal. Chem.* **2009**, *81*, 1275−9. (c) Zheng, G.; Patolsky, F.; Cui, Y.; Wang, W. U.; Lieber, C. M. *Nat. Biotechnol.* **2005**, *23*, 1294−1301.

(6) For a review see, for example: de Mel, A.; Jell, G.; Stevens, M. M.; Seifalian, A. M. *Biomacromolecules* **2008**, *9*, 2969−79.

(7) (a) Kuhl, P. R.; Griffith-Cima, L. G. *Nat. Med.* **1996**, *2*, 1022−7. (b) Richardson, T. P.; Peters, M. C.; Ennett, A. B.; Mooney, D. J. *Nat. Biotechnol.* **2001**, *19*, 1029−32.

(8) (a) Chen, Y.-X.; Triola, G.; Waldmann, H. *Acc. Chem. Res.* **2011**, *44*, 762−73. (b) Wong, L. S.; Khan, F.; Micklefield, J. *Chem. Rev.* **2009**, *109*, 4025−53. (c) Rusmini, F.; Zhong, Z. Y.; Feijen, J. *Biomacromolecules* **2007**, *8*, 1775−89. (d) Speers, A. E.; Cravatt, B. F. *ChemBioChem* **2004**, *5*, 41−7. (e) Jonkheijm, P.; Weinrich, D.; Schroeder, H.; Niemeyer, C. M.; Waldmann, H. *Angew. Chem., Int. Ed.* **2008**, *47*, 9618−47.

(9) (a) Soellner, M. B.; Dickson, K. A.; Nilsson, B. L.; Raines, R. T. *J. Am. Chem. Soc.* **2003**, *125*, 11790−1. (b) Watzke, A.; Koehn, M.; Gutierrez-Rodriguez, M.; Wacker, R.; Schroeder, H.; Breinbauer, R.; Kuhlmann, J.; Alexandrov, K.; Niemeyer, C. N.; Goody, R. S.; Waldmann, H. *Angew. Chem., Int. Ed.* **2006**, *45*, 1408−12. (c) de Araujo, A. D.; Palomo, J. M.; Cramer, J.; Kohn, M.; Schroder, H.; Wacker, R.; Niemeyer, C.; Alexandrov, K.; Waldmann, H. *Angew. Chem., Int. Ed.* **2006**, *45*, 296−301. (d) Duckworth, B. P.; Xu, J. H.; Taton, T. A.; Guo, A.; Distefano, M. *Bioconjugate Chem.* **2006**, *17*, 967−74. (e) Lin, P. C.; Ueng, S. H.; Tseng, M. C.; Ko, J. L.; Huang, K. T.; Yu, S. C.; Adak, A. K.; Cheng, Y. J.; Lin, C. C. *Angew. Chem., Int. Ed.* **2006**, *45*, 4286−90. (f) Govindaraju, T.; Jonkheijm, P.; Gogolin, L.; Schroeder, H.; Becker, C. F. W.; Niemeyer, C. M.; Waldmann, H. *Chem. Commun.* **2008**, 3723−5. (g) Christman, K. L.; Broyer, R. M.; Tolstyka, Z. P.; Maynard, H. D. *J. Mater. Chem.* **2007**, *17*, 2021−7. (h) Lempens, E. H. E.; Helms, B. A.; Merkx, M.; Meijer, E. W. *ChemBioChem* **2009**, *10*, 658−62. (i) Zhang, K.; Diehl, M. R.; Tirrell, D. A. *J. Am. Chem. Soc.* **2005**, *127*, 10136−7. (j) Weinrich, D.; Lin, P. C.; Jonkheijm, P.; Nguyen, U. T. T.; Schroder, H.; Niemeyer, C. M.; Alexandrov, K.; Goody, R. S.; Waldmann, H. *Angew. Chem., Int. Ed.* **2010**, *49*, 1252−7. (k) Hodneland, C. D.; Lee, Y.-S.; Min, D.-H.; Mrksich, M. *Proc. Natl. Acad. Sci. U.S.A.* **2002**, *99*, 5048−52. (l) Kindermann, M.; George, N.; Johnsson, N.; Johnsson, K. *J. Am. Chem. Soc.* **2003**, *125*, 7810−1.

(10) (a) Aida, T.; Meijer, E. W.; Stupp, S. I. *Science* **2012**, *335*, 813−7. (b) Fenske, T.; Korth, H.-G.; Mohr, A.; Schmuck, C. *Chem.—Eur. J.* **2012**, *18*, 738−55. (c) Uhlenheuer, D. A.; Petkau, K.; Brunsveld, L. *Chem. Soc. Rev.* **2010**, *39*, 2817−26. (d) Sacca, B.; Niemeyer, C. M. *Angew. Chem., Int. Ed.* **2012**, *51*, 58−66. (e) Mager, M. D.; LaPointe, V.; Stevens, M. M. *Nat. Chem.* **2011**, *3*, 582−9. (f) Rybtschinski, B. *ACS Nano* **2011**, *5*, 6791−818.

(11) (a) Jun, H. W.; Yuwono, V.; Paramonov, S. E.; Hartgerink, J. D. *Adv. Mater.* **2005**, *17*, 2612−7. (b) Nallur, S. K. M.; Voskuhl, J.; Bultema, J. B.; Boekema, E. J.; Ravoo, B. J. *Angew. Chem., Int. Ed.* **2011**, *50*, 9747−51. (c) Lee, D.-W.; Park, K. M.; Banerjee, M.; Ha, S. H.; Lee, T.; Suh, K.; Paul, S.; Jung, H.; Kim, J.; Selvapalam, N.; Ryu, S. H.; Kim, K. *Nat. Chem.* **2011**, *3*, 154−9. (d) Kim, C.; Agasti, S. S.; Zhu, Z.; Isaacs, L.; Rotello, V. M. *Nat. Chem.* **2010**, *2*, 962−66. (e) Liu, Y.; Wang, H.; Kamei, K. I.; Yan, M.; Chen, K.-J.; Yuan, Q.; Shi, L.; Lu, Y.; Tseng, H.-R. *Angew. Chem., Int. Ed.* **2011**, *50*, 3058−62. (f) Meyer, R.; Niemeyer, C. M. *Small* **2011**, *7*, 3211−8. (g) Shah, R. N.; Shah, R. A.; Del Rosario Lim, M. M.; Hsieh, C.; Nuber, G.; Stupp, S. I. *Proc. Natl. Acad. Sci. U.S.A.* **2010**, *107*, 3293−8. (h) Dankers, P. Y. W.; Harmsen, M. C.; Brouwer, L. A.; Luyn, M. J. A.; Meijer, E. W. *Nat. Mater.* **2005**, *4*, 568−74. (I) Krogman, K. C.; Lowery, J. L.; Zacharia, N. S.; Rutledge, G. C.; Hammond, P. T. *Nat. Mater.* **2009**, *8*, 512−8.

(12) (a) Zhu, H.; Bilgin, M.; Bangham, R.; Hall, D.; Casamayor, A.; Bertone, P.; Lan, N.; Jansen, R.; Bidlingmaier, S.; Houfek, T.; Mitchell, T.; Miller, P.; Dean, R. A.; Gerstein, M.; Snyder, M. *Science* **2001**, *293*, 2101−5. (b) Becker, C. F. W.; Wacker, R.; Bouschen, W.; Seidel, R.; Kolaric, B.; Lang, P.; Schroeder, H.; Mueller, O.; Niemeyer, C. M.; Spengler, B.; Goody, R. S.; Engelhard, M. *Angew. Chem., Int. Ed.* **2005**, *44*, 7635−9. (c) Hutschenreiter, S.; Tinazli, A.; Model, K.; Tampé, R. *EMBO J.* **2004**, *44*, 2488−97. (d) Kwon, Y.; Coleman, M. A.; Camarero, J. A. *Angew. Chem., Int. Ed.* **2006**, *45*, 1726−9. (e) Escalante, M.; Zhao, Y.; Ludden, M. J. W.; Vermeij, R.; Olsen, J. D.; Berenschot, E.; Hunter, C. N.; Huskens, J.; Subramaniam, V.; Otto, C. *J. Am. Chem. Soc.* **2008**, *130*, 8892−3. (f) Hwang, I.; Baek, K.; Jung, M.; Kim, Y.; Park, K. M.; Lee, D.-W.; Selvapalam, N.; Kim, K. *J. Am. Chem. Soc.* **2007**, *129*, 4170−1. (g) Camarero, J. A. *Pept. Sci.* **2007**, *90*, 450−8. (h) Young, J. F.; Nguyen, H. D.; Yang, L.; Huskens, J.; Jonkheijm, P.; Brunsveld, L. *ChemBioChem* **2010**, *11*, 180−3. (i) Uhlenheuer, D. A.; Wasserberg, D.; Haase, C.; Nguyen, H. D.; Schenkel, J. H.; Huskens, J.; Ravoo, B. J.; Jonkheijm, P.; Brunsveld, L. *Chem.—Eur. J.* **2012**, *18*, 6788−94. (j) Ludden, M. J. W.; Mulder, A.; Tampé, R.; Reinhoudt, D. N.; Huskens, J. *Angew. Chem., Int. Ed.* **2007**, *46*, 4104−7. (k) Gonzalez-Campo, A.; Eker, B.; Gardeniers, H. J. G. E.; Huskens, J.; Jonkheijm, P. *Small* **2012**, DOI: 10.1002/smll.201200565. (l) Kolodziej, C. M.; Chang, C.-W.; Maynard, H. D. *J. Mater. Chem.* **2011**, *21*, 1457−61.

(13) (a) Grunwald, C.; Schulze, K.; Reichel, A.; Weiss, V. U.; Blaas, D.; Piehler, J.; Weismüller, K.-H.; Tampé, R. *Proc. Natl. Acad. Sci. U.S.A.* **2010**, *107*, 6146−51. (b) Hyun, J.; Lee, W.-K.; Chilkoti, A.; Zauscher, S. *J. Am. Chem. Soc.* **2004**, *126*, 7330−5. (c) Wan, P. B.; Wang, Y. P.; Jiang, Y. G.; Xu, H. P.; Zhang, X. *Adv. Mater.* **2009**, *21*, 4362−5. (d) Arumugam, S.; Popik, V. V. *J. Am. Chem. Soc.* **2012**, *134*, 8408−11.

(14) (a) Mrksich, M. *Chem. Soc. Rev.* **2000**, *29*, 267−73. (b) Pulsipher, A.; Yousaf, M. N. *ChemBioChem* **2010**, *11*, 745−53. (c) Yousaf, M. N. *Curr. Opin. Chem. Biol.* **2009**, *13*, 697−704. (d) Robertus, J.; Browne, W. R.; Feringa, B. L. *Chem. Soc. Rev.* **2010**, *39*, 354. (e) Mrksich, M. *Curr. Opin. Chem. Biol.* **2002**, *6*, 794−7. (f) Mendes, P. *Chem. Soc. Rev.* **2008**, *37*, 2512−29.

(15) (a) Ciampi, S.; James, M.; Le Saux, G.; Gaus, K.; Gooding, J. J. *J. Am. Chem. Soc.* **2012**, *134*, 844−7. (b) Chen, E. W. L.; Park, S.; Yousaf, M. N. *Angew. Chem., Int. Ed.* **2008**, *47*, 6267−71. (c) Luo, W.; Chan, E. W. L.; Yousaf, M. N. *J. Am. Chem. Soc.* **2010**, *132*, 2614−21. (d) Chen, Z.; Li, Y.; Liu, W.; Zhang, D.; Zhao, Y.; Yuan, B.; Jiang, X. *Angew. Chem., Int. Ed.* **2009**, *48*, 8303−5. (e) Wildt, B.; Wirtz, D.; Searson, P. C. *Nat. Methods* **2009**, *6*, 211−3.
(16) (a) Haddour, N.; Cosnier, S.; Gondran, C. *J. Am. Chem. Soc.* **2005**, *127*, 5752−3. (b) Agarwal, G.; Naik, R. R.; Stone, M. O. *J. Am. Chem. Soc.* **2003**, *125*, 7408−12. (c) Hodneland, C. D.; Mrksich, M. *J. Am. Chem. Soc.* **2000**, *122*, 4235−6.
(17) (a) Ong, W.; Kaifer, A. E. *Organometallics* **2003**, *22*, 4181−3. (b) Jeon, W. S.; Moon, K.; Park, S. H.; Chun, H.; Ko, Y. H.; Lee, J. Y.; Lee, E. S.; Samal, S.; Selvapalam, N.; Rekharsky, M. V.; Sindelar, V.; Sobransingh, D.; Inoue, Y.; Kaifer, A. E.; Kim, K. *J. Am. Chem. Soc.* **2005**, *127*, 12984−9.
(18) (a) Kaifer, A. E. *Acc. Chem. Res.* **1999**, *32*, 62−71. (b) Nijhuis, C. A.; Ravoo, B. J.; Huskens, J.; Reinhoudt, D. N. *Coord. Chem. Rev.* **2007**, *251*, 1761−80.
(19) Dubacheva, G. V.; Van Der Heyden, A.; Dumy, P.; Kaftan, O.; Auzéley-Velty, R.; Coche-Guerente, L.; Labbé, P. *Langmuir* **2010**, *26*, 13976−86.
(20) Nijhuis, C. A.; Huskens, J.; Reinhoudt, D. N. *J. Am. Chem. Soc.* **2004**, *126*, 12266−7.
(21) Chen, Y. F.; Banerjee, I. A.; Yu, L.; Djalali, R.; Matsui, H. *Langmuir* **2004**, *20*, 8409−13.
(22) Dubacheva, G. V.; Galibert, M.; Coche-Guerente, L.; Dumy, P.; Boturyn, D.; Labbé, P. *Chem. Commun.* **2011**, *47*, 3565−7.
(23) Uhlenheuer, D. A.; Wasserberg, D.; Nguyen, H.; Zhang, L.; Blum, C.; Subramaniam, V.; Brunsveld, L. *Chem.—Eur. J.* **2009**, *15*, 8779−90.
(24) Craik, D. J. *Nat. Chem.* **2012**, *4*, 600−2.
(25) (a) Beulen, M. W. J.; Bugler, J.; Lammerink, B.; Geurts, F. A. J.; Biemond, E.; van Leerdam, K. G. C.; van Veggel, F.; Engbersen, J. F. J.; Reinhoudt, D. N. *Langmuir* **1998**, *14*, 6424−9. (b) Beulen, M. W. J.; Bugler, J.; de Jong, M. R.; Lammerink, B.; Huskens, J.; Schonherr, H.; Vancso, G. J.; Boukamp, B. A.; Wieder, H.; Offenhauser, A.; Knoll, W.; van Veggel, F.; Reinhoudt, D. N. *Chem.—Eur. J.* **2000**, *6*, 1176−83.
(26) Rekharsky, M. V.; Inoue, Y. *Chem. Rev.* **1998**, *98*, 1875−917.
(27) (a) Castro, R.; Cuadrado, I.; Alonso, B.; Casado, C. M.; Moran, M.; Kaifer, A. E. *J. Am. Chem. Soc.* **1997**, *119*, 5760−1. (b) Auletta, T.; de Jong, M. R.; Mulder, A.; van Veggel, F. J. C. M.; Huskens, J.; Reinhoudt, D. N.; Zou, S.; Zapotoczny, S.; Schönherr, H.; Vancso, G. J.; Kuipers, L. *J. Am. Chem. Soc.* **2004**, *126*, 1577−84.
(28) Mulder, A.; Auletta, T.; Sartori, A.; Del Ciotto, S.; Casnati, A.; Ungaro, R.; Huskens, J.; Reinhoudt, D. N. *J. Am. Chem. Soc.* **2004**, *126*, 6627−36.
(29) Wendeln, C.; Ravoo, B. J. *Langmuir* **2012**, *28*, 5527−38.
(30) (a) Wachter, R. M.; Yarbrough, D.; Kallio, K.; Remington, S. J. *J. Mol. Biol.* **2000**, *301*, 157−71. (b) Shaner, N. C.; Patterson, G. H.; Davidson, M. W. *J. Cell Sci.* **2007**, *120*, 4247−60.
(31) Cottrell, F. G. *Z. Phys. Chem.* **1903**, *42*, 385−431.
(32) An, Q.; Brinkmann, J.; Huskens, J.; Krabbenborg, S.; de Boer, J.; Jonkheijm, P. *Angew. Chem., Int. Ed.* **2012**, DOI: 10.1002/anie.201205651.